2016 IEEE 55th Conference on Decision and Control (CDC)
ARIA Resort & Casino
December 12-14, 2016, Las Vegas, USA

State Estimation of Wastewater Treatment Processes Using Distributed Extended Kalman Filters

Jing Zeng, Jinfeng Liu, Tao Zou and Decheng Yuan

Abstract— **In this work, we develop a distributed state estimation scheme for wastewater treatment processes in the context of extended Kalman filtering. Specifically, we consider a wastewater treatment process that includes a five-compartment reactor and an ideal splitter. First, we present a method to design the sensor network for the process and then discuss how the process may be decomposed into subsystems for distributed state estimation. We present a detailed design of the distributed filters and a detailed distributed state estimation algorithm to coordinate the actions of the different filters. The distributed scheme is compared with a centralized extended Kalman filtering scheme under dry weather conditions. Simulation results show that the distributed scheme can give comparable estimation performance to the centralized scheme or even better performance than the centralized scheme. Also, the distributed estimation scheme is shown to have more stable performance under different noise conditions.**

I. Introduction

Wastewater treatment is an important step in water recycle and it involves complex biological and physical phenomena. A wastewater treatment plant (WWTP) is typically a large scale nonlinear system including a series of biological reactors and a settler. The effluent quality is closely related to the sustainability of environment and normally is regulated by environmental legislations. Because the influent flow and the composition in the flow to a WWTP usually vary significantly which pose significant challenges in the associated control system design.

Different process control schemes have been reported for WWTPs including proportional-integral (PI) control [1], [2], model predictive control (MPC) [3]–[6] and economic MPC [7]. While there are many results on the control system design for WWTPs, relatively less attention has been given to the state estimation of WWTPs. State estimation is a process of constructing system states based on output measurements and a system model. State estimation is closely related to the control and monitoring of WWTPs and is an important topic in the operation of WWTPs since many relevant states in wastewater treatment are not measurable or are subject to significant noise. Two commonly used state estimation methods for nonlinear systems are the extended Kalman filter (EKF) [8] and the moving horizon state estimation (MHE) [9]. To handle nonlinearity, in EKF, successive linearization of the nonlinear system is performed every sampling time. The MHE is an optimization-based state estimator that can handle nonlinear systems and system constraints. However, MHE is usually very computationally demanding especially for nonlinear systems. In [10], both EKF and MHE were applied to the state estimation of a WWTP. It was shown that both the EKF and the MHE can give good estimation performance even under difficult conditions. Since the EKF and MHE gives similar performance, EKF was recommended due to its simplest and efficiency in implementation. In [10], the EKF was implemented in a centralized framework. For large-scale systems, centralized implementation is not favorable from a fault-tolerance as well as maintenance points of view [11].

Motivated by the above consideration, in this work, we propose a distributed state estimation scheme for WWTPs in the context of EKF. The proposed distributed state estimation provides an alternative scheme to the centralized estimation scheme and is inspired by our previous work on distributed MHE [12], [13]. Specifically, in this work, we consider a typical wastewater treatment process that includes a five-compartment reactor and an ideal splitter. First, we propose a method for sensor network design and subsystem decomposition for distributed state estimation; and then we present the detailed design of the distributed EKFs. A detailed distributed state estimation algorithm is also introduced to coordinate the actions of the different EKFs. Without loss of generality, we consider the entire system is decomposed into two subsystems. The proposed approach can be extended in a straightforward fashion to include more subsystems. The distributed EKF scheme is compared with a centralized EKF under dry weather conditions.

II. Wastewater treatment processes

The Benchmark Simulation Model No.1 (BSM1) is composed of a five-compartment activated sludge reactor and a secondary settler, which is a popular benchmark for evaluating different control strategies for WWTP. In this work, the process model is based on BSM1 benchmark and the plant layout is shown in Figure 1 [10], [14]. The five sludge reactors in BSM1 remain unchanged while the secondary settler is replaced by a membrane filtration unit, which is modeled as an ideal splitter [10]. The activated sludge reactor section includes two anoxic compartments (anoxic section) and three aerobic compartments (aerated section). In this

Financial support from the National Natural Science Foundation of China (61503257 & 61374112), the Natural Science Foundation of Liaoning Province, China (2014020138), the Program for Liaoning Province Distinguished Young Scholars in University (LJQ2014045) and the University of Alberta (RES0014908) is acknowledged.

Jing Zeng and Decheng Yuan are with Liaoning Province Key Laboratory of Control Technology for Chemical Processes, Shenyang University of Chemical Technology, Shenyang, 110142, China. Jinfeng Liu is with the Department of Chemical & Materials Engineering, University of Alberta, Edmonton, AB T6G 2V4, Canada. Tao Zou is with Shenyang Institute of Automation, Chinese Academy of Sciences, Shenyang, 110016, China. Corresponding author: J. Liu. Email: jinfeng@ualberta.ca.

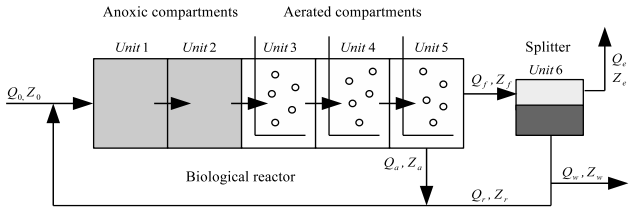

Fig. 1. General overview of the modified BSM1.

process, two elementary reactions take place in the two different sections: denitrification biological reactions take place in the anoxic section where bacteria change nitrate into nitrogen; and nitrification reactions in which the bacteria oxidize ammonium to nitrate take place in the aerated section. Wastewater is feed into the first anoxic reactor at flow rate Q_0 and concentration Z_0 [1]. A portion of the effluent of the last aerated reactor is recycled back to the first anoxic reactor at flow rate Q_a and concentration Z_a (i.e., internal recycle) with the rest of the effluent is fed into the splitter at flow rate Q_f and concentration Z_f. The processed water leaves from the top of the splitter at flow rate Q_e and concentration Z_e. The generated sludge is withdrawn from the bottom of the splitter at flow rate Q_w and concentration Z_w. A second recycle stream from the splitter is fed back to the first anoxic reactor at flow rate Q_r and concentration Z_r (i.e., external recycle).

The biological phenomena taking place in the five biological compartments are described by the Activated Sludge Model no. 1 (ASM1) [14]. In the simulation model, eight biological processes are used to describe the biological behavior, 13 different compounds are considered and the concentrations of these compounds are the state variables of the simulation model. The definitions of these state variables are given in Table I. A total of 78 ordinary differential equations are used to described the dynamics of the entire plant in which each biological reactor and the splitter are described by 13 ordinary differential equations according to the the 13 state variables.

In the model, the general equations of biological reactor (i.e., two anoxic reactors and three aerated reactors) on mass balances are as follows [14]:

For $k = 1$ (reactor 1):

$$\frac{dZ_1}{dt} = \frac{1}{V_1}(Q_a Z_a + Q_r Z_r + Q_0 Z_0 + r_1 V_1 - Q_1 Z_1) \tag{1a}$$

$$Q_1 = Q_a + Q_r + Q_0 \tag{1b}$$

For $k = 2$ to 5 (reactor 2 to 5):

$$\frac{dZ_k}{dt} = \frac{1}{V_k}(Q_{k-1} Z_{k-1} + r_k V_k - Q_k Z_k) \tag{2a}$$

$$Q_k = Q_{k-1} \tag{2b}$$

[1]A generic compound Z is used in the description to denote the different compounds (see Table 2) in the wastewater treatment plant to simplify the description.

TABLE I

LIST OF STATE VARIABLES

Notation	Definition	Unit
S_I	Soluble inert organic matter	$gCOD/m^3$
S_S	Readily biodegradable substrate	$gCOD/m^3$
X_I	Particulate inert organic matter	$gCOD/m^3$
X_S	Slowly biodegradable substrate	$gCOD/m^3$
$X_{B,H}$	Active heterotrophic biomass	$gCOD/m^3$
$X_{B,A}$	Active autotrophic biomass	$gCOD/m^3$
X_P	Particulate products from biomass decay	$gCOD/m^3$
S_O	Oxygen	$g(-COD)/m^3$
S_{NO}	Nitrate and nitrite nitrogen	gN/m^3
S_{NH}	NH_4^+ and NH_3 nitrogen	gN/m^3
S_{ND}	Soluble biodegradable organic nitrogen	gN/m^3
X_{ND}	Particulate biodegradable organic nitrogen	gN/m^3
S_{ALK}	Alkalinity	mol/m^3

Special case for oxygen ($S_{O,k}$)

$$\frac{dS_{O,k}}{dt} = \frac{1}{V_k}(Q_{k-1} S_{O,k-1} + r_k V_k + (K_L a)_k V_k (S_O^* - S_{O,k}) - Q_k S_{O,k}) \tag{3}$$

where the saturation concentration for oxygen is $S_O^* = 8g.m^{-3}$, r_k denotes the observed conversion rates of different compounds in reactor k, the detail calculation of r_k can be found in [14].

As for the splitter, assuming there is no biological activity in it, the equations of mass balances is as follows:

For $k = 6$ (splitter):

Soluble compounds (i.e., S_I, S_S, S_O, S_{NO}, S_{NH}, S_{ND}, S_{ALK}):

$$\frac{dZ_k}{dt} = \frac{1}{V_k}(Q_f Z_{k-1} + (Q_e + Q_r + Q_w) Z_k) \tag{4}$$

Note that for the well-mixed soluble compounds in the splitter, the concentrations of Z_e, Z_r, Z_w for every soluble compound (S_I, S_S, S_O, S_{NO}, S_{NH}, S_{ND}, S_{ALK}) are all the same and is indicated as Z_k $(k = 6)$. Moreover, the concentrations of the seven soluble compounds in the last aerated reactor is equal to the corresponding concentrations in the splitter, which means $Z_{k-1} = Z_k$ $(k = 6)$ in (4).

Solid compounds (i.e., X_I, X_S, $X_{B,H}$, $X_{B,A}$, X_P, X_{ND}):

$$\frac{dZ_k}{dt} = \frac{1}{V_k}(Q_f Z_{k-1} + (Q_r + Q_w) Z_k) \tag{5}$$

In the ideal splitter, we suppose that all the six solid compounds precipitate in the bottom of the basin, so the concentration Z_e at the top of the splitter for the solid compounds are all zeros. The concentrations Z_r and Z_w are the same and can be described as Z_k $(k = 6)$.

The flow rates of the plant layout in Figure 1 satisfy the following equations:

$$\begin{aligned} &Q_1 = Q_2 = Q_3 = Q_4 = Q_5 \\ &Q_1 = Q_a + Q_r + Q_0 \\ &Q_f = Q_5 - Q_a = Q_e + Q_r + Q_w = Q_e + Q_u \\ &Q_0 = Q_e + Q_w \end{aligned} \tag{6}$$

The above model of the WWTP can be described in a

compact form as follows:

$$\dot{x}(t) = f(x(t), u(t), w(t)) \tag{7a}$$
$$y(t) = Cx(t) + v(t) \tag{7b}$$

where $x \in \mathbb{R}^{78}$ is the vector of process state variables, w denotes random process noise/disturbances not explicitly described by the model, u denotes the manipulated input vector, y is the measured output vector and v is a measurement noise vector. In this work, we propose a systematic approach for the design of distributed extended Kalman filters (EKF) for the WWTP. We will divide the entire WWTP into two subsystems and for each subsystem, a local EKF is designed. The two EKFs communicate with each other and collaboratively estimate the entire states of the WWTP. The propose approach can be applied to the design of distributed state estimation schemes with more subsystems.

III. Subsystem configuration

In this section, the WWTP system will be decomposed into two subsystems for the purpose of distributed state estimation. In subsystem decomposition, the primary factor considered is the observability of the subsystem and the entire system. In addition to the observability consideration, we follow the following guidelines: (a) subsystem decomposition aligns with the system's physical topology is more favorable and (b) an operating unit in the WWTP is preferred to be associated with only one local estimator.

A. Available measurements

In the WWTP, there are in total 48 states that can be measured using commercially available instruments [10]. For each of the five biological reactors and the ideal splitter, eight state variables or state related variables can be measured. They are: (1) concentration of oxygen S_O, (2) concentration of alkalinity S_{ALK}, (3) concentration of ammonia S_{NH}, (4) concentration of nitrate S_{NO}, (5) chemical oxygen demand COD, (6) filtered chemical oxygen demand COD_f, (7) biological oxygen demand BOD, and (8) total suspended solids TSS. The definitions and expressions of these available measurements are given in Table II.

TABLE II
List of measured outputs

Notation	Definition	Expression
S_O	Oxygen	S_O
S_{ALK}	Alkalinity	S_{ALK}
S_{NH}	NH_4^+ and NH_3 nitrogen	S_{NH}
S_{NO}	Nitrate and nitrite nitrogen	S_{NO}
COD	Chemical oxygen demand	$S_I + S_S + X_S + X_I + X_{B,H} + X_{B,A}$
COD_f	Filtered COD	$S_I + S_S$
BOD	Biological oxygen demand	$S_S + X_S$
TSS	Total suspended solids	$X_I + X_S + X_{B,H} + X_{B,A} + X_P + X_{ND}$

B. Sensor network design and subsystem decomposition

In the wastewater treatment plant, to design a state estimation system, a prerequisite is that the entire plant and the two subsystems are observable. A system is said to be observable if, for a time interval $[t_0, t_1]$, given the input and output measurements over the interval it is possible to solve for the initial state $x(t_0)$ [15]. The WWTP is a nonlinear process. In order to check its observability, we linearize the nonlinear model at different points along typical state trajectories and check the observability of these linearized models. This approximation approach was also used in [10]. The linear approximation of the process at $x(t)$ can be described as the following form (assuming zero process and measurement noise without loss of generality):

$$\begin{aligned} \dot{x}(t) &= A(t)x(t) + B(t)u(t) \\ y(t) &= C(t)x(t) \end{aligned} \tag{8}$$

where $A(t)$ and $C(t)$ are obtained by taking the Jacobian of (7a) and (7b) at $x(t)$ respectively. There are different approaches to carry out observability test. In this work, we use the Popov-Belevich-Hautus (PBH) rank test to check the observability of the WWTP. The observability test is to check if the observability matrix O_k $(k = 1, ...n)$ has a full column rank:

$$rank(O_k) = n, \quad k = 1, ..., n \tag{9}$$

where

$$O_k = \begin{bmatrix} \lambda_k I - A \\ C \end{bmatrix}, \quad k = 1, ..., n \tag{10}$$

where n is the number of differential states, which is also the dimension of A, λ_k is the kth eigenvalue of A and I is the identity matrix. If the linear approximation is observable at all the selected points along the typical state trajectories, the nonlinear system is also observable in neighborhoods of the typical trajectories.

In a distributed framework, the subsystem observability should be checked before performing distributed state estimation. For subsystem i, its observability is checked based on the pair (A_{ii}, C_i) which are the corresponding blocks in A and C to subsystem i. We first test the observability of the five biological rectors and the ideal splitter based on different sets of measurements. It is found that the entire states of each of the biological reactor can be observed based on a few of the measurements of the same reactor. However, the splitter is not observable based only on the measurements of the splitter itself. It is also found that the states of the splitter are observable based on a combination of measurements of the splitter itself and the measurements of reactor 1. In order to achieve a balance in terms of number of states, the entire WWTP is decomposed into two subsystems as follows:

(1) Subsystem 1: Ideal splitter and Anoxic compartments (reactor 1 and reactor 2);
(2) Subsystem 2: Aerated compartments (reactor 3, reactor 4 and reactor 5).

Each subsystem model contains 39 state variables and 24 measurements. The balanced number of state variables in the two subsystems makes the decomposition more favorable than others from a computational and communicational points of view. Once the subsystem decomposition is determined, observability tests are performed for each subsystems based on different combination of the measure-

ments to determine a minimum set of measurements that ensures observability of the subsystem. The minimum sets of measurements for the two subsystem are found to be:

(1) Subsystem 1:
Ideal splitter: COD_6, $S_{ALK,6}$;
Reactor 2: COD_2, $COD_{f,2}$, TSS_2, $S_{O,2}$, $S_{ALK,2}$
(2) Subsystem 2:
Reactor 3: COD_3, $COD_{f,3}$, TSS_3, $S_{ALK,3}$.

We should also check the observability of the entire system again based on the measurements of the two subsystems. Note that the above minimum sets of measurements ensure the observability of the subsystems and the entire system. However, in order to have robust performance in the distributed state estimation design in the presence of process disturbances and measurement noise, it is recommended that some easy-to-measure measurements are added to the minimum sets to increase the robustness of the estimation method [10]. In this work, the nitrate and ammonia measurements in the effluent ($S_{NO,6}$, $S_{NH,6}$) are added into subsystem 1; the measurements of oxygen in the aerated reactors (SO_3, SO_4 and SO_5) are added into subsystem 2.

IV. Distributed EKF design

A. Design of subsystem filters

In this work, the distributed extended Kalman filters are designed. We denote the vectors of the state variables of the two subsystems as x_1 and x_2 respectively, and denote the vectors of measured outputs as y_1 and y_2 respectively. The two subsystems can be described as the following forms:

$$\dot{x}_1(t) = f_1(x_1(t), x_2(t), u(t), w_1(t)) \tag{11a}$$
$$y_1(t) = C_1 x_1(t) + v_1(t) \tag{11b}$$
$$\dot{x}_2(t) = f_2(x_1(t), x_2(t), u(t), w_2(t)) \tag{11c}$$
$$y_2(t) = C_2 x_2(t) + v_2(t) \tag{11d}$$

where w_1 and w_2 are the process noise, v_1 and v_2 are the measurement noise in their respective subsystems. Note that the two subsystems are coupled via their states.

Extended Kalman filters are discrete time filters for nonlinear systems based on successive linearization of the nonlinear system. EKF consists of a prediction step and an update step. Past data is processed and propagated by means of a suitable statistics. In the design of distributed EKF, each subsystem is associated with a local EKF which is evaluated at every sampling time t_k. The EKF associated with subsystem i ($i = 1,2$) will be referred to as EKF i and it is designed as follows:

(1) Prediction step:

$$\hat{x}_i(t_k|t_{k-1}) = \hat{x}_i(t_{k-1}) + \int_{t_{k-1}}^{t_k} f_i(\hat{x}_1(t), \hat{x}_2(t), u(t), 0)dt \tag{12a}$$
$$P_i(t_k|t_{k-1}) = A_i(t_{k-1}) P_i(t_{k-1}) A_i(t_{k-1})^T + Q_i \tag{12b}$$

(2) Update step:

$$K_i(t_k) = P_i(t_k|t_{k-1}) C_i^T (C_i P_i(t_k|t_{k-1}) C_i^T + R_i)^{-1} \tag{13a}$$
$$\hat{x}_i(t_k) = \hat{x}_i(t_k|t_{k-1}) + K_i(t_k)(y_i(t_k) - C_i \hat{x}_i(t_k|t_{k-1})) \tag{13b}$$
$$P_i(t_k) = (I - K_i(t_k) C_i) P_i(t_k|t_{k-1}) \tag{13c}$$

where (12a) and (12b) are prediction steps, (13a), (13b) and (13c) are update steps. $\hat{x}_i(t_k|t_{k-1})$ denotes the prediction of the state at time instant t_k based on the state estimate $\hat{x}_i(t_{k-1})$ at t_{k-1} and subsystem model f_i, $P_i(t_{k-1})$ describe the error covariance matrix of $\hat{x}_i(t_{k-1})$, $P_i(t_k|t_{k-1})$ predicts the error covariance matrix at time t_k based on the corresponding value at t_{k-1}. The matrices Q_i and R_i denote the covariances of process disturbance and measurement noise of subsystem i, respectively. $A_i(t_{k-1})$ is the Jacobians of f_i with respect to x_i at time t_{k-1} and $K_i(t_k)$ is the filter gain at t_k. Based on (12a), it can be seen that EKF i needs information of both subsystem states (i.e., x_1 and x_2). This implies that the two distributed EKFs need to communicate to exchange their state estimates. The distributed estimation algorithm below describes the detailed implementation of the distributed EKFs.

B. Distributed state estimation algorithm

We assumed that each local EKF has immediate access to the output measurements of its associated subsystem and it can also communicate with the other subsystem to exchange their subsystem state estimates. The exchanged information is used to compensate for the interactions between the two subsystems in order to improve their state estimates.

The proposed distributed EKF scheme uses the following algorithm to carry out the state estimation of the WWTP:

Algorithm 1: Distributed extend Kalman filter algorithm

1) At $t_0 = 0$, the two EKFs are initialized with the initial subsystem state guesses $\hat{x}_i(0)$, $i = 1,2$, and the subsystem output measurements $y_i(0)$, $i = 1,2$.
2) At $t_k > 0$, carry out the following steps:
   2.1. EKF i receives $y_i(t_k)$, $i = 1,2$.
   2.2. Each EKF receives the subsystem state estimates of the previous time instant from the other subsystem; that is, EKF i ($i = 1,2$) receives $\hat{x}_j(t_{k-1})$, $j = 1,2$, $j \neq i$.
   2.3. Based on both the local measurement and information from other subsystems, each EKF calculates the estimate of its subsystem's state; that is, EKF i calculates $\hat{x}_i(t_k)$, $i = 1,2$.
   2.4. EKF i sends the current information (i.e., $\hat{x}_i(t_k)$, $i = 1,2$) to the other subsystems.
3) Go to Step 2 at the next sampling time t_{k+1}.

Note that the process input information (i.e., $u(t)$) is assumed to be known to both of the EKFs. Note also that in the prediction step of EKF i at t_k, $\hat{x}_j(t_{k-1})$ is used to approximate $x_j(t)$ for $t \in [t_{k-1}, t_k)$ in (12a).

V. Simulations

In this section, we apply the distributed EKF scheme to the WWTP and compare its estimation performance with a centralized EKF under dry weather conditions. The data file can be found in the International Water Association website [16]. The file contains two weeks of dynamic dry weather influent data, we do the simulations only for the first week. In the simulations, it is assumed that the entire process measurements are sampled synchronously and periodically, and Δ =15 min is the sampling time interval. In every set of

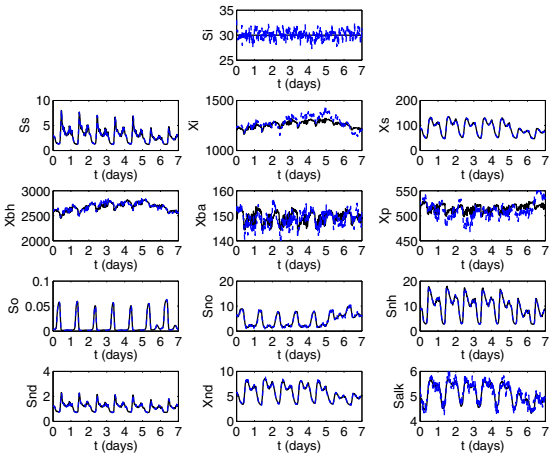

Fig. 2. Trajectories of the actual process state (solid lines) and the estimates given by the EKF (dashed lines) of reactor 1.

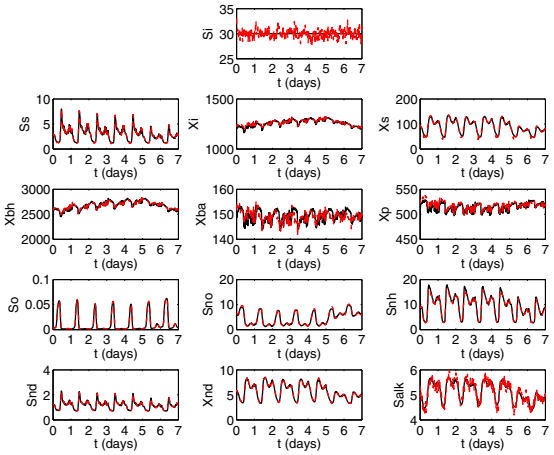

Fig. 3. Trajectories of the actual process state (solid lines) and the estimates given by the distributed EKF (dashed lines) of reactor 1.

simulations, the same noise sequences and initial conditions are used in both schemes.

In the first set of simulations, the random process disturbances in the dynamics of the 78 states are generated with the zero mean, standard deviation vector being $0.2x_0$ and bounded between $-0.2x_0$ and $0.2x_0$; the bounded noise in the measurements is generated as normally distributed values with zero mean, standard deviation $0.2y_0$ and the values are restricted to be in the interval $[-0.2y_0,\ 0.2y_0]$, where x_0 denotes the initial conditions and y_0 can be calculated by $y_0 = Cx_0$. The initial guess in the different estimation schemes is set to be $1.1x_0$. The parameters used in the EKF are $Q = diag((0.2x_0)^2)$, $R = diag((0.2y_0)^2)$ and $P(0) = Q = diag((0.2x_0)^2)$ where the notation $diag(v)$ represents a diagonal matrix whose diagonal elements are the elements of a vector v. For the distributed EKF, the parameters of the two subsystems are: $Q_i = diag((0.2x_{0,i})^2)$, $R_i = diag((0.2y_{0,i})^2)$ and $P_i(0) = Q_i = diag((0.2x_{0,i})^2)$, where $x_{0,i}$ and $y_{0,i}$ are the corresponding portion in x_0 and y_0 to subsystem i, $i = 1,2$.

Figure 2 shows the actual state trajectories and the estimates of reactor 1 given by the centralized EKF. Figure 3 shows the actual state trajectories and the estimates of reactor 1 obtained using the distributed EKF. From the figures, it can be seen that both the EKF and the proposed distributed EKF can track the trend of the actual system states well. To compare the performance of the EKF and the distributed EKF, we calculate the errors given by the two schemes. To account for the different magnitudes of the estimation errors for different states, the error for each state is normalized based on its maximum estimation error from the two estimation schemes. The Euclidean norms of the normalized estimation error is defined as: $e(t_k) = \sqrt{\sum_{i=1}^{78} (e_i(t_k))^2}$, where $e(t_k)$ is the normalized error at time instant t_k. $e_i(t_k)$ is the normalized error of state i, $i = 1,2,...,78$, defined as:

$$e_i(t_k) = \frac{\hat{x}_i(t_k) - x_i(t_k)}{max(\hat{x}_i - x_i)} \tag{14}$$

where the maximum error for a given state i is the largest error for state i among the EKF and the distributed EKF.

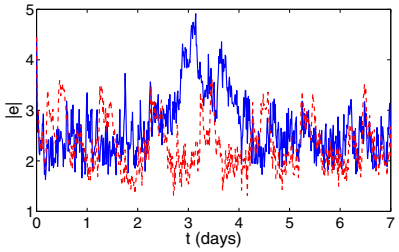

Fig. 4. Trajectories of the Euclidean norm of normalized estimation errors given by the EKF (solid lines) and the distributed EKF (dashed lines).

The mean values of the normalized estimation error is defined as: $Mean|e| = \frac{1}{K}\sum_{k=1}^{K} e(t_k)$, where K is the total number of samples over simulation period. Based on the simulation results, the mean values of the estimation errors over the seven days given by the centralized EKF and the distributed EKF are 2.7214 and 2.4144, respectively. The maximum values of estimation errors calculated by the EKF and the distributed EKF are 4.9174 and 4.5590, respectively. In this particular simulation, with the distributed EKF, there are approximately 11% and 7% improvements with respect to the centralized EKF in terms of mean and maximum estimation error. Figure 4 shows the trajectories of the Euclidean norms of the normalized estimation errors given by the two different schemes. We would like to note that there is no guarantee that the centralized scheme should give a better performance than the distributed scheme when EKF is applied to a nonlinear process.

In another set of simulations, the effect of process disturbance and measurement noise on the performance of the centralized EKF and the distributed EKF is studied. In this set of simulations, the same initial guess $1.1x_0$ as in the first set of simulations is used but with different process disturbance and measurement noise. We suppose the process noise is Gaussian white noise generated with the zero mean, standard deviation $w_Q x_0$ and bounded between $-w_Q x_0$ and $w_Q x_0$, and the parameter Q used in the centralized EKF is

TABLE III

PERFORMANCE COMPARISON UNDER THE DRY WEATHER

	w_R	w_Q	Centralized	Distributed
Mean$\|e\|$	0.3	0.3	2.7826	2.3735
	0.25	0.25	2.3345	2.0770
	0.2	0.2	1.8849	1.7950
	0.1	0.1	0.9592	1.3068
	0.05	0.05	0.4930	1.1370
Max$\|e\|$	0.3	0.3	4.9416	3.6426
	0.25	0.25	4.1486	3.4277
	0.2	0.2	3.3270	3.2330
	0.1	0.1	1.6446	3.0924
	0.05	0.05	0.8134	3.0920
CPU time			1.82s	1.03s

$Q = diag((w_Q x_0)^2)$. In the distributed EKF, Q_i is set to be $Q_i = diag((w_Q x_{0,i})^2)$, $i = 1,2$. The measurement noise is generated with zero mean, standard deviation being $w_R y_0$ and bounded between $-w_R y_0$ and $w_R y_0$, the corresponding parameter R used in the centralized EKF is $R = diag((w_R y_0)^2)$, $P(0)$ is set to be the same as Q. In the distributed EKF, $R_i = diag((w_R y_{0,i})^2)$ and $P_i(0) = Q_i = diag((w_Q x_{0,i})^2)$.

The mean and maximum of the norm of the normalized estimation errors given by the EKF and the distributed EKF with different process disturbance and measurement noise are shown in Table III. Note that in order to compare the performance given by different w_Q and w_R, the maximum error for a given state i in Eq.(14) is the largest error for state i among all the EKF and the distributed EKF in this set of simulations. For this reason, the mean and maximum of the combination $w_Q = w_R = 0.2$ are different from the ones reported in the first set of simulations. From Table III, it can be seen that the centralized EKF is more sensitive to the properties of the noise sequences. The overall trend is that the performance of the centralized EKF decreases obviously with the increase of the magnitude of the noise. However, the distributed EKF has a relatively more stable performance in terms of mean and maximum error under these different noise realizations. When the noise is small, the centralized EKF overall gives better performance; when the noise is increased, the distributed EKF may give better performance.

From the simulations, we found that the distributed EKF has a relatively more stable performance under different noise realizations. One possible explanation is that in the distributed framework, the noise of a subsystem is restricted to be within the subsystem and is essentially isolated from the other subsystem. While in the centralized framework, the noise of one subsystem is propagated into the other subsystem via the centralized model. This also implies that the distributed EKF has the potential to give a better performance in terms of fault tolerance. Regarding the average CPU times, it can be seen from Table III that the evaluation time of the distributed EKF is significant (43%) less than the centralized EKF. Note that all the simulations are carried out in MATLAB using an Intel Core i5 Computer at 1.80GHz with 4GB RAM.

VI. CONCLUSIONS

In this work, we developed a distributed EKF scheme for the wastewater treatment process and compared its estimation performance with a centralized EKF. A benchmark simulation model based on BSM1 was used to simulate the WWTP under dry weather conditions. The simulations results demonstrated that the distributed EKF has improved estimation performance compared to the centralized EKF in the case of large disturbance noise and measurement noise. The results also showed the distributed EKF has a rather stable performance than the centralized EKF in term of mean error under different noise realizations, which implies the distributed EKF has the potential to give a better performance in terms of fault tolerance. In addition, the evaluation time given by the distributed EKF is significant less than the centralized EKF.

REFERENCES

[1] V. C. Machado, D. Gabriel, J. Lafuente, and J. A. Baeza. Cost and effluent quality controller design based on the relative gain array for a nutrient removal WWTP. *Water Research*, 43:5129–5141, 2009.

[2] A. Araujo, S. Gallani, M. Mulas, and G. Olsson. Systematic approach to the design of operation and control policies in activated sludge systems. *Industrial & Engineering Chemistry Research*, 54:8542–8557, 2011.

[3] M. O'Brien, J. Mack, B. Lennox, D. Lovett, and A. Wall. Model predictive control of an activated sludage process: A case study. *Control Engineering Practice*, 19:54–61, 2011.

[4] M. Francisco, P. Vega, and S. Revollar. Model predictive control of BSM1 benchmark of wastewater treatment process: a tuning procedure. In *50th IEEE Conference on Decision and Control and European Control Conference*, Orlando, FL, USA, 2011.

[5] H. G. Han, X. L. Wu, and J. F. Qiao. Nonlinear model-predictive control for industrial processes: an application to wastewater treatment process. *IEEE Transactions on Industrial Electronics*, 61:1970–1980, 2014.

[6] P. Vega, S. Revollar, M. Francisco, and J. M. Martin. Integration of set point optimization techniques into nonlinear MPC for improving the opration of WWTPs. *Computers and Chemical Engineering*, 68:78–95, 2014.

[7] J. Zeng and J. Liu. Economic model predictive control of wastewater treatment processes. *Industrial & Engineering Chemistry Research*, 54:5710–5721, 2015.

[8] G. A. Einicke. *Smoothing, filtering and prediction: estimating the past, present and future*. Intech, Croatia, 2012.

[9] D. G. Robertson, J. H. Lee, and J. B. Rawlings. A moving horizon-based approach for least-squares estimation. *AIChE Journal*, 42:2209–2224, 1996.

[10] J. Busch, D. Elixmann, P. Kuhl, C. Gerkens, J. P. Schloder, H. G. Bock, and W. Marquardt. State estimation for large-scale wastewater treatment plants. *Water Research*, 47:4774–4787, 2013.

[11] P. D. Christofides, R. Scattolini, D. Muñoz de la Peña, and J. Liu. Distributed model predictive control: A tutorial review and future research directions. *Computers & Chemical Engineering*, 51:21–41, 2013.

[12] J. Zhang and J. Liu. Distributed moving horizon estimation for nonlinear systems with bounded uncertainties. *Journal of Process Control*, 23:1281–1295, 2013.

[13] J. Zeng and J. Liu. Distributed moving horizon state estimation: Simultaneously handling communication delays and data losses. *Systems & Control Letters*, 75:56–68, 2015.

[14] J. Alex, L. Benedetti, J. Copp, K. V. Gernaey, U. Jeppsson, I. Nopens, M. N. Pons, L. Rieger, C. Rosen, J. P. Steyer, P. Vanrolleghem, and S. Winkler. Benchmark simulation model no.1 (BSM1). Technical report, Department of Industrial Electrical Engineering and Automation, Lund University, 2008.

[15] C. Chen. *Linear System Theory and Design*. Oxford University Press, USA, 4th edition, 2012.

[16] International Water Association. http://www.benchmarkwwtp.org.